Supporting Information

Polyanion Electrolytes with Well-Ordered Ionic Layers in Simulations and Experiment

Lauren J. Abbott,[*,†] Hilda G. Buss,[‡,¶] Jacob L. Thelen,[‡,§] Bryan D. McCloskey,[*,‡,¶] and John W. Lawson[‖]

†*AMA Inc., Thermal Protection Materials Branch, NASA Ames Research Center, Moffett Field, California 94035, United States*

‡*Department of Chemical and Biomolecular Engineering, University of California, Berkeley, California 94720, United States*

¶*Energy Storage and Distributed Resources Division, Lawrence Berkeley National Laboratory, Berkeley, California 94720, United States*

§*Materials Sciences Division, Lawrence Berkeley National Laboratory, Berkeley, California 94720, United States*

‖*Thermal Protection Materials Branch, NASA Ames Research Center, Moffett Field, California 94035, United States*

E-mail: lauren.j.abbott@nasa.gov; bmcclosk@berkeley.edu

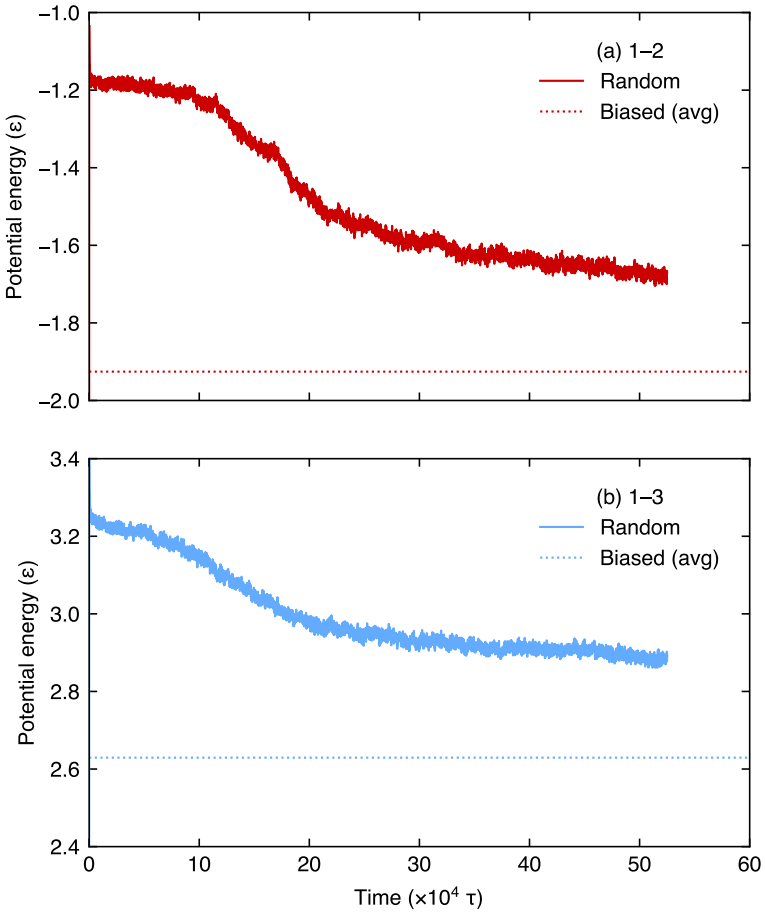

Figure S1: Potential energies per bead, U_{pot}, for the (a) 1–2 and (b) 1–3 models. Solid lines give the instantaneous energy as a function of time for the random models, while dashed lines mark the mean energy for the equilibrated biased models.

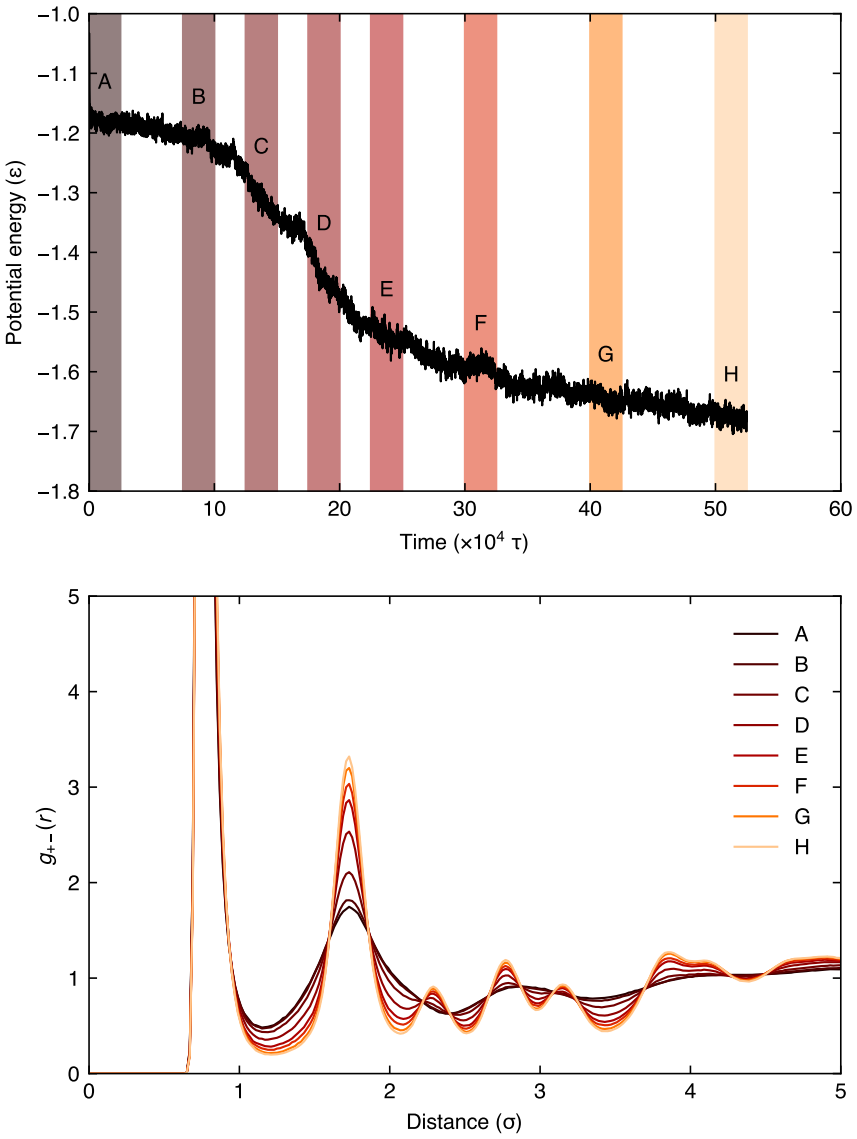

Figure S2: Potential energy per bead, U_{pot}, (top) and cation–anion radial distribution functions, $g_{+-}(r)$, (bottom) calculated during simulations of the 1–2 random model. The radial distribution functions were averaged over the shaded regions marked in the energy plot with the corresponding labels A–H.

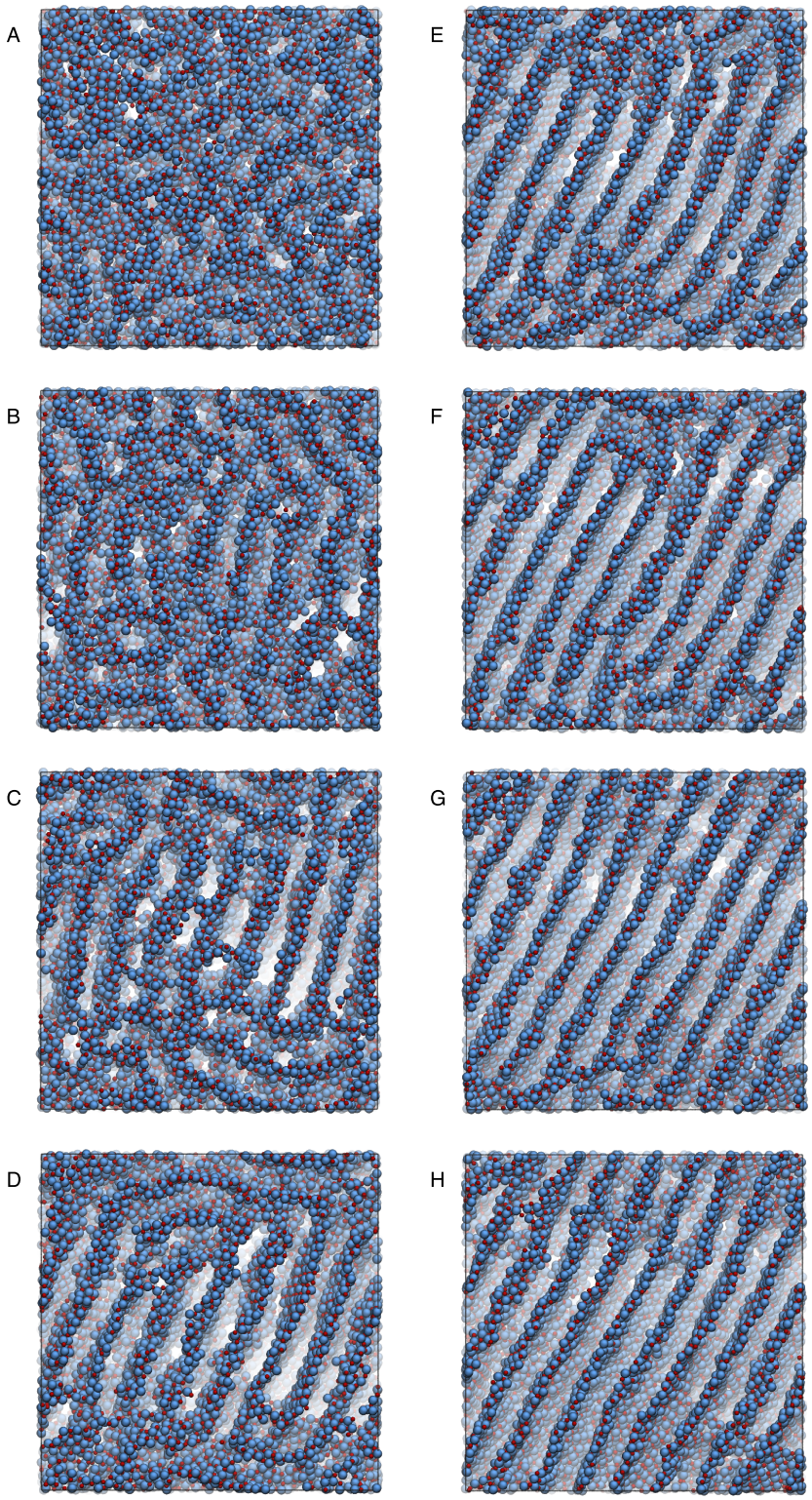

Figure S3: Snapshots taken from simulations of the 1–2 random model. Specifically, the snapshots were taken from the end of the shaded regions marked in the energy plot in Figure S2 with the corresponding labels A–H. Anion beads are shown in blue and cation beads in red, while all remaining polymer beads are not shown for clarity.

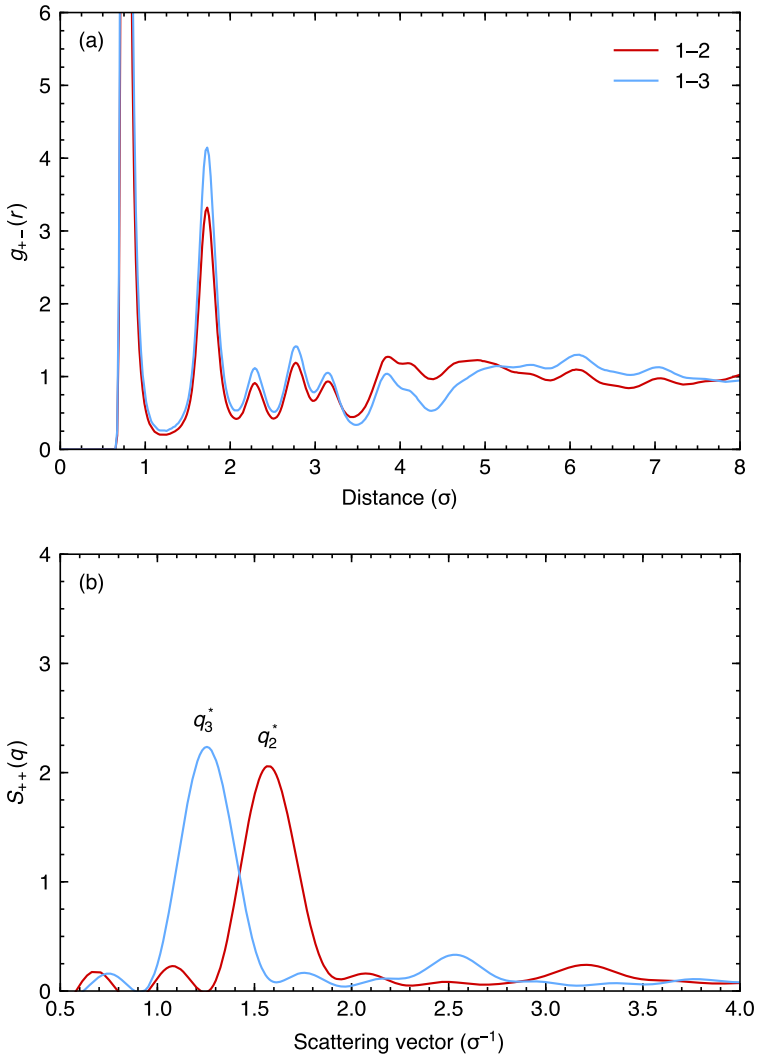

Figure S4: (a) Cation–anion radial distribution functions, $g_{+-}(r)$, and (b) cation–cation partial structure factors, $S_{++}(q)$, for the 1–2 and 1–3 random models. The peaks in (b) corresponding to the lamellar domain spacings are marked q_2^* and q_3^* for the 1–2 and 1–3 systems, respectively.

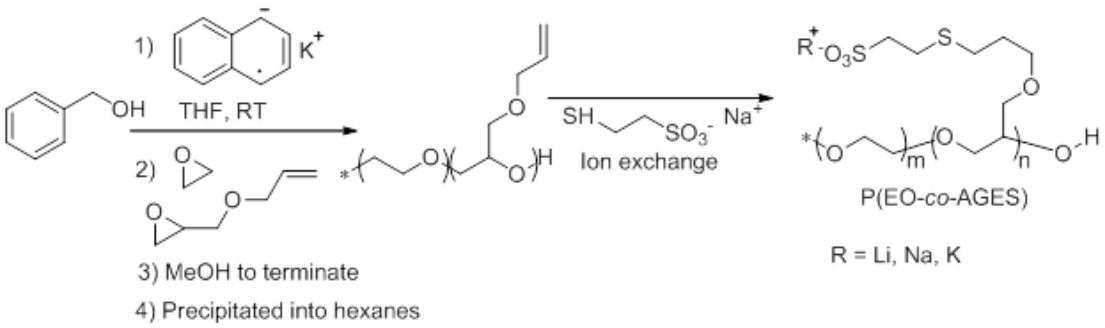

Figure S5: Synthesis scheme of P(EO-co-AGES) copolymers.

Table S1: Molecular weight of precursor polymers

	GPC[a]			NMR
AGE (mol %)	M_n[b] (kDa)	M_w[c] (kDa)	D[d]	M_n (kDa)
100	18	21	1.1	21
69	14	17	1.2	13
50	15	17	1.2	14
33	20	25	1.3	15

[a]Polystyrene standard; [b]Number average molecular weight;
[c]Weight average molecular weight; [d]Polydispersity

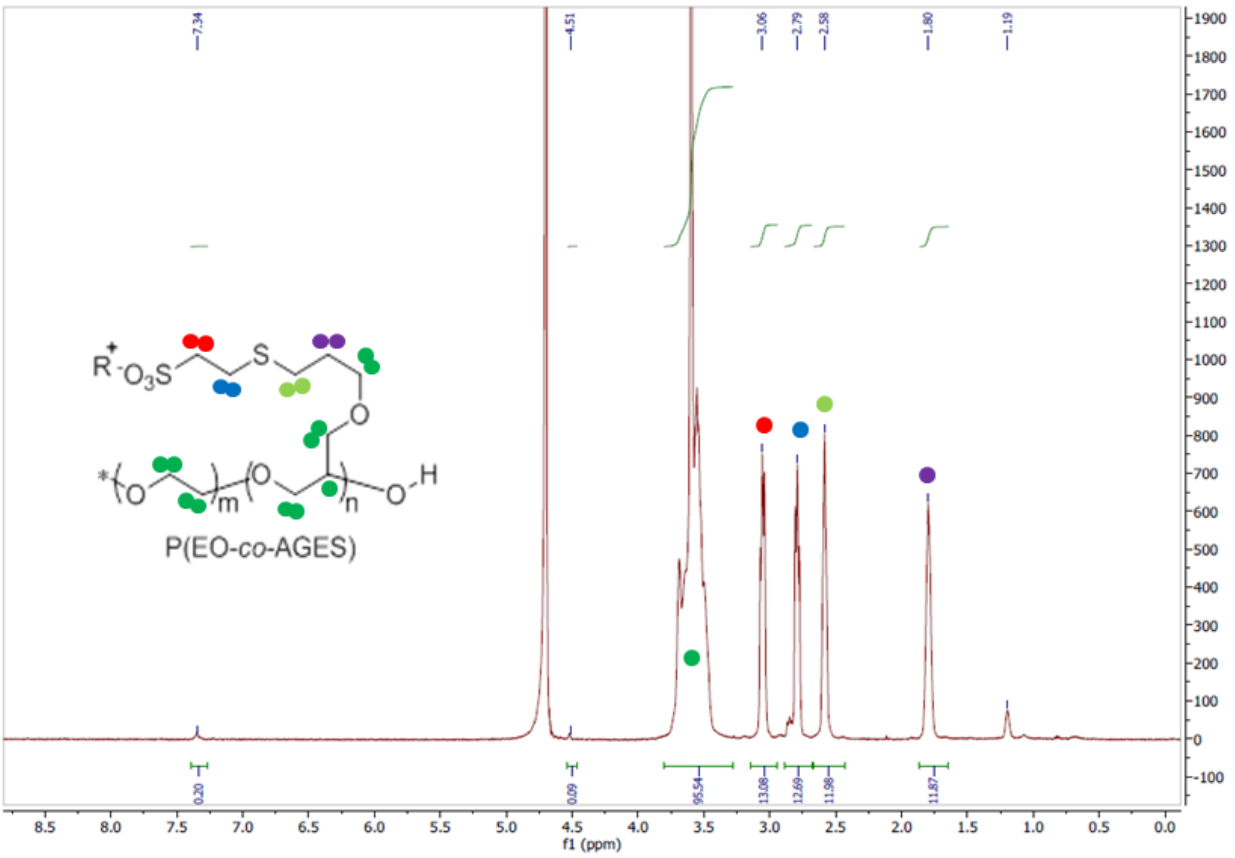

Figure S6: NMR spectrum of P(EO-*co*-AGES) with 33 mol % AGES. Peak assignments are indicated by the colored beads. The peak at 7.34 ppm is associated with the 4 protons off the initiator's benzyl ring and used for end group analysis. The peak at 1.19 ppm is due to an isomer of the AGE, which is still able to participate in the click reaction.

Table S2: ICP-OES of ion exchanged polymers

AGES (mol %)	Counter ion	ICP-OES (ppm)[a]			
		K	Li	Na	S[b]
100	Na	0 (0)	0 (0)	16.2 (1.3)	72.9 (0)
100	Li	0.1 (0.1)	12.3 (0.6)	0.9 (0.3)	
69	Li	0.5 (0.1)	6.4 (0.2)	1.1 (0.2)	70.2 (3.1)
69	Na	0.7 (0.1)	0 (0)	19.5 (0.9)	69.7 (5.8)
69	K	26 (1.5)	0 (0)	0.8 (0.2)	76.5 (7.4)
50	Na	0.2 (0.1)	0 (0)	19.9 (2.2)	
50	Li	0.1 (0)	8.2 (0.2)	4.9 (0.2)	
33	Na	0.6 ()	0 ()	59.0 ()	

[a]The number reported is the average over three different wavelengths calibrated for that element, while the standard deviation is reported in parentheses. Empty values were not recorded. [b]The presence of sulfur is due to the sulfide linkage.

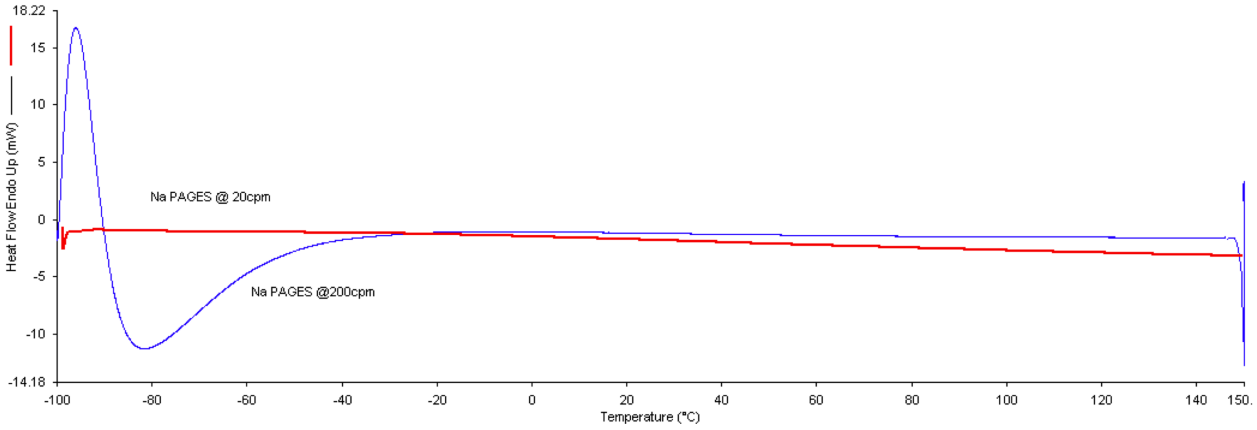

Figure S7: DSC thermal analysis of Na-PAGES at both fast and slow heating rates. The second heating scan is shown in each case. The fast cooling trace has larger artifacts at the beginning and end of the scan, but can increase the size of glass transitions, making them easier to observe. No accessible phase transitions are observed.

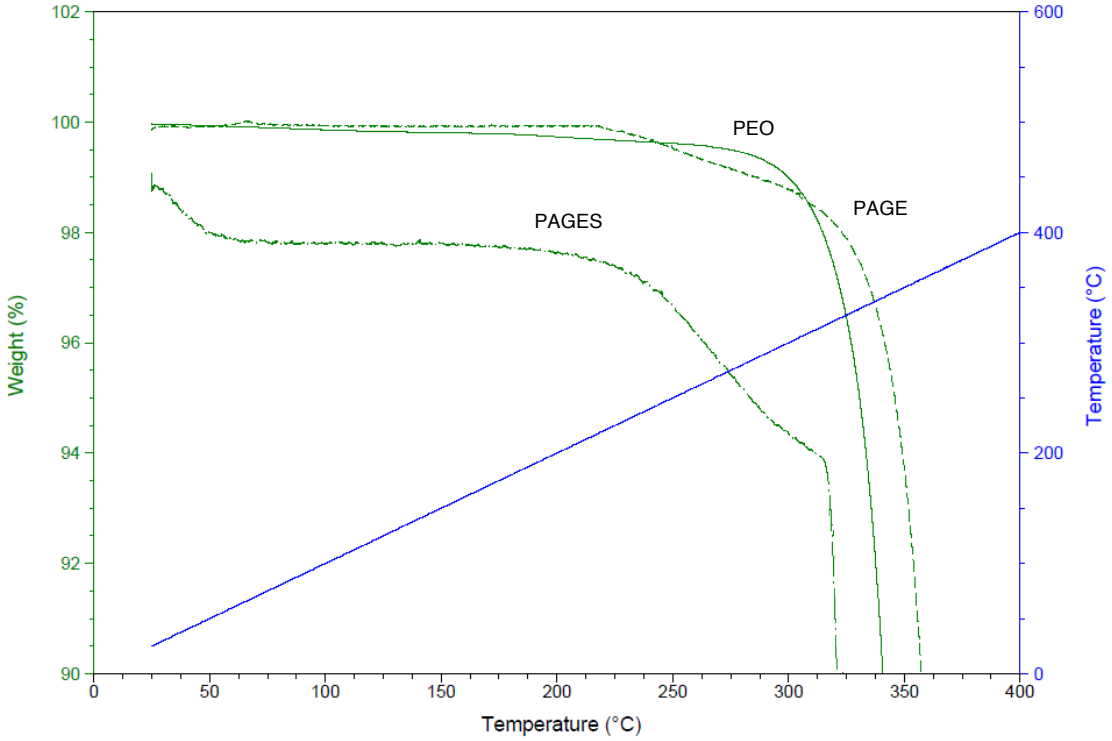

Figure S8: TGA plot of PEO, parent polymer PAGE, and sulfonated polymer PAGES. The ion content of the PAGES polymer makes it very hygroscopic. The initial drop in mass at the start of the scan is due to initial water loss.

(a) Schematic

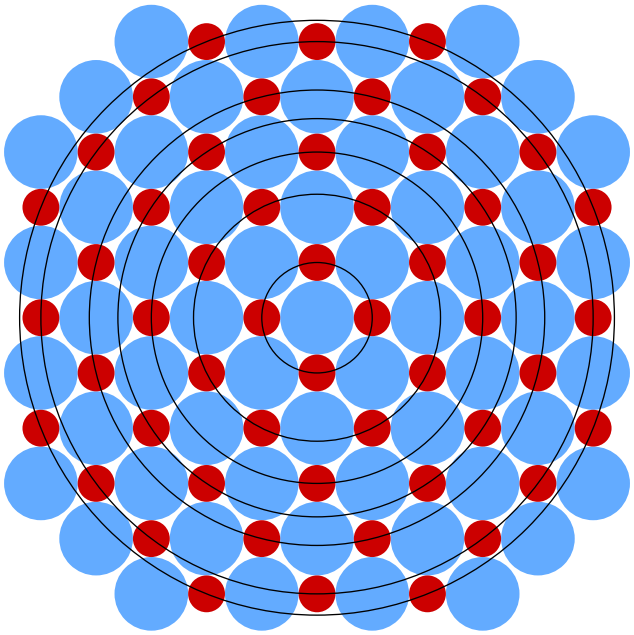

(b) 1–2, biased

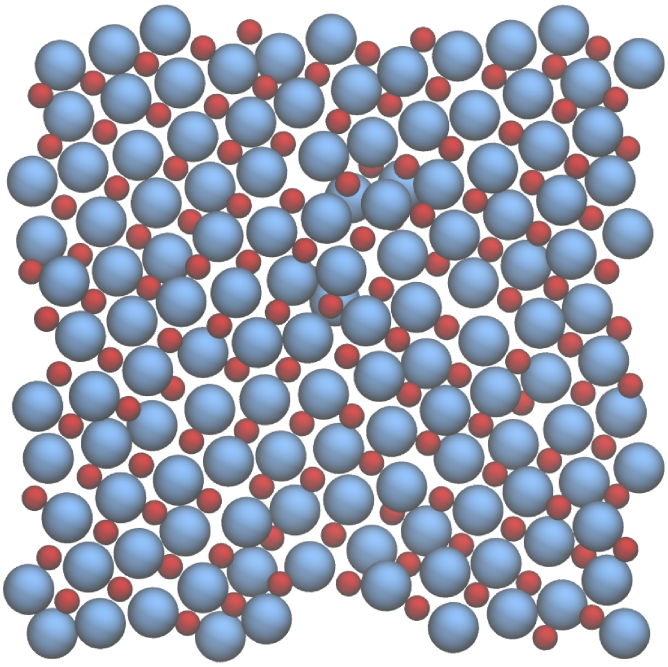

Figure S9: (a) Schematic of a single-layer NaCl-like ordering of cations and anions. Cations and anions are given in red and blue, respectively. Black circles mark the first seven coordination layers. (b) Snapshot of part of an ionic layer formed in the 1–2 random model.

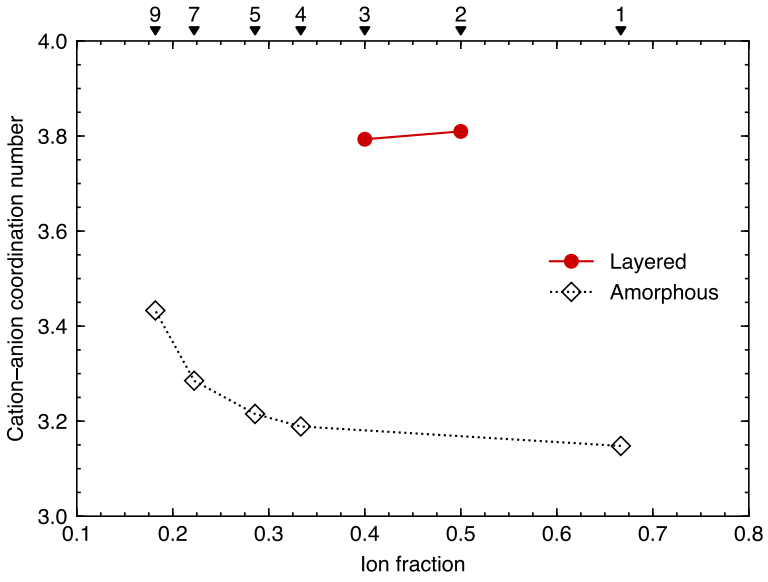

Figure S10: Average cation–anion coordination numbers, $\bar{n}_{+-}$, for the (a) 1–2 and (b) 1–3 biased models with layered ionic morphologies compared with bead-spring models with amorphous ordering of ionic aggregates from previous work.[S1] The arrows above the plot indicate the number of side chain beads in the model at the corresponding ion fraction.

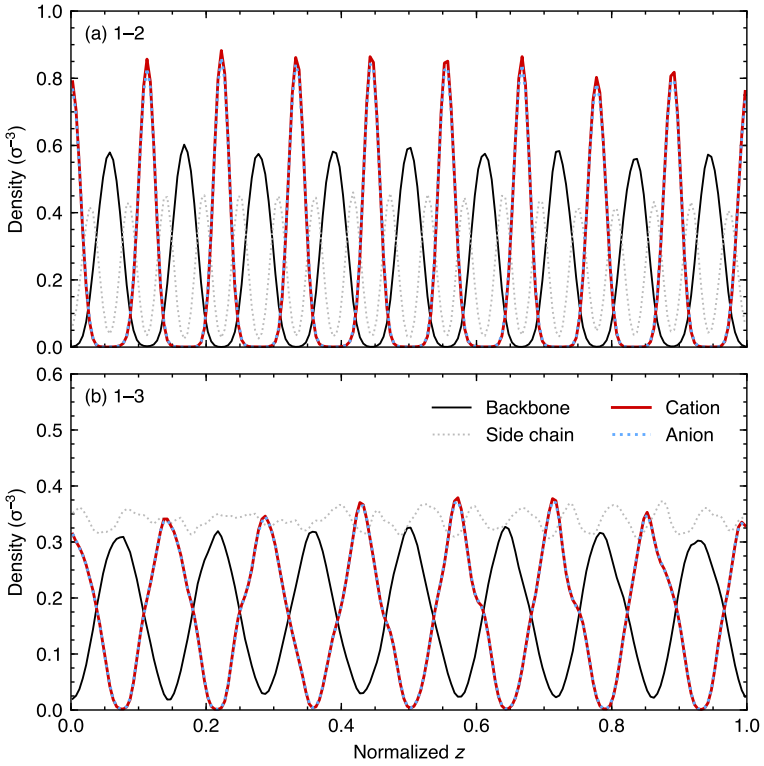

Figure S11: Density profiles in the z-dimension, $\rho(z)$, given as a function of the z-coordinate normalized by the box length in the z-dimension, z/L_z, for the polymer backbone, polymer side chain, cation, and anion beads in the (a) 1–2 and (b) 1–3 biased models. Note that the cation and anion profiles are almost identical.

Table S3: X-ray scattering peak positions

Peak	q (nm^{-1})	q/q^*	d (nm)
q^*	2.476	1.000	2.538
$2q^*$	4.956	2.002	1.268
$3q^*$	7.428	3.000	0.846
$4q^*$	9.898	3.998	0.635
$5q^*$	12.404	5.010	0.507
$6q^*$	14.822	5.986	0.424
$7q^*$	17.304	6.989	0.363
$8q^*$	19.751	7.977	0.318
$9q^*$	22.264	8.992	0.282
$10q^*$	24.678	9.967	0.255
$11q^*$	27.665	11.173	0.227

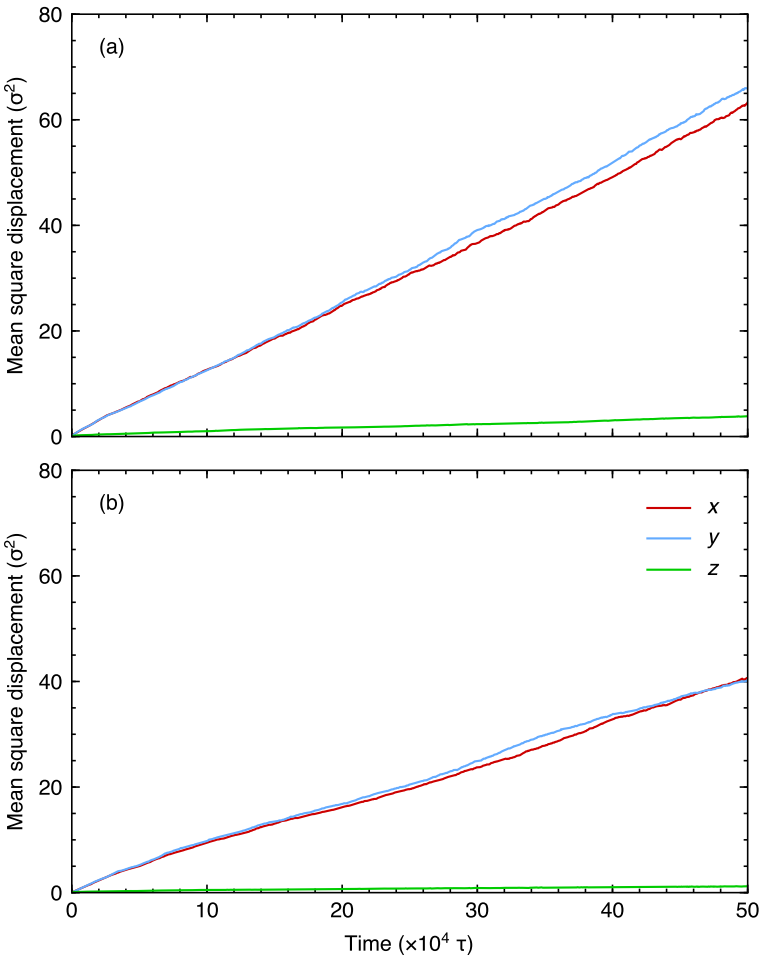

Figure S12: Cation mean square displacements, $\left\langle (r_i(t) - r_i(0))^2 \right\rangle$, in the x-, y-, and z-dimensions for the (a) 1–2 and (b) 1–3 biased models. Note that the ionic layers are stacked in the z-direction.

References

[S1] Abbott, L. J.; Lawson, J. W. Effects of Side Chain Length on Ionic Aggregation in Polymer Single-Ion Conductors. *Macromolecules*, submitted for publication.